A&A 424, 355–361 (2004)
DOI: 10.1051/0004-6361:20041017

Astronomy & Astrophysics

Oscillator strengths for transitions to Rydberg levels in $^{12}C^{16}O$, $^{13}C^{16}O$ and $^{13}C^{18}O$ between 967 and 972 Å⋆

M. Eidelsberg[1], J. L. Lemaire[1,2], J. H. Fillion[1,2], F. Rostas[1], S. R. Federman[3], and Y. Sheffer[3]

[1] LERMA, UMR 8112 du CNRS, Observatoire de Paris, 92195 Meudon Cedex, France
e-mail: michele.eidelsberg@obspm.fr
[2] LERMA/LAMAp, UMR 8112 du CNRS, Université de Cergy-Pontoise, 95031 Cergy-Pontoise, France
[3] Department of Physics and Astronomy, University of Toledo, Toledo, Ohio 43606, USA

Received 3 April 2004 / Accepted 11 May 2004

Abstract. Absorption oscillator strengths have been determined from high-resolution spectra in the 967–972 Å region of three CO isotopomers for transitions to the Rydberg levels 4pπ(0), 3dπ(1) and 4pσ(0), as well as to the mixed *E(6)* level recently characterized by Eidelsberg et al. (2004). Synchrotron radiation from the Super-ACO electron storage ring at Orsay (LURE) was used as a light source. Oscillator strengths were extracted from the recorded spectra by least-squares fitting of the experimental profiles with synthetic spectra taking into account the homogeneous and heterogeneous interactions of the four levels. Column densities were derived from fits to the 3pπ(0) absorption band whose oscillator strength is well established. These are the first reported measurements for $^{13}C^{18}O$. For $^{12}C^{16}O$, our results are consistent with the larger values obtained in the most recent laboratory and astronomical studies.

Key words. ISM: molecules – methods: laboratory – molecular data – ultraviolet: ISM

1. Introduction

The column density of CO and its isotopomers in diffuse interstellar clouds is derived from vacuum ultraviolet (VUV) absorption bands seen in spectra acquired with the *Hubble Space Telescope (HST)* and the *Far Ultraviolet Spectroscopic Explorer (FUSE)*. Such absorption is the only technique providing direct access to the column density. However, the accuracy of the results obtained is entirely dependent on that of the band and line oscillator strengths used in the data reduction. Over the years, data on oscillator strengths provided by laboratory measurements have improved and many discrepancies have been resolved. In particular, a set of recommended values for the $A-X$ band oscillator strengths has been proposed on the basis of converging experimental and theoretical results (Eidelsberg et al. 1999). These bands cover the 1300–1600 Å region and six orders of magnitude in oscillator strength. In the same wavelength range, the triplet-singlet intersystem bands are typically 2 to 6 orders of magnitude weaker and can be used for dense clouds where the $A-X$ bands are optically thick. The large discrepancies that initially appeared between observed and predicted oscillator strengths for these transitions (Federman et al. 1994; Sheffer et al. 2002) have been resolved thanks to a new theoretical model that allows a reliable calculation of band and line oscillator strengths (Rostas et al. 2000; Eidelsberg & Rostas 2003).

The availability of FUSE has extended the accessible wavelength range to the 905–1187 Å region where CO absorbs through transitions from the ground state to Rydberg states such as $B^1\Sigma^+$, $C^1\Sigma^+$, $E^1\Pi$, etc. The oscillator strengths for these transitions have often been measured in the laboratory but significant differences still exist between the sets of results. The available laboratory data have been reviewed by Federman et al. (2001) and Sheffer et al. (2003) and compared by the latter to their recent FUSE results. These comparisons clearly show that the available results for bands below 1075 Å still show too much scatter to provide a consensus which could lead to a set of recommended f-values for use in VUV measurements and in modelling CO photochemistry in astronomical environments.

In the light of this situation, the availability of the new SU5 high resolution beam line on the Super-ACO synchrotron at Orsay has allowed us to undertake a systematic study of the absorption cross sections for Rydberg bands starting with the $3p\pi^1\Pi(E)$–$X^1\Sigma^+(0–0)$ band at 1076 Å and up to the W–$X(3–0)$ band at 925 Å. Taking advantage of the full rotational resolution seen in most cases by the 30 mÅ (even 20 mÅ in the best cases) instrumental width, we used the simulation-fitting technique to analyse the spectra. This technique generally can account for overlapping of adjacent bands and for effects of line saturation which may appear in strong and sharp features.

We present here a sample of the results obtained for three isotopomers, $^{12}C^{16}O$, $^{13}C^{16}O$ and $^{13}C^{18}O$. The focus is on a spectral region where three or four bands associated with the Rydberg levels 4pσ(0), 4pπ(0) and 3dπ(1) (formerly $K(0)$, $L(0)$

⋆ Based on experiments done at the Super-ACO electron storage ring at Orsay (LURE), France.

and $L'(1)$ and with the $E(6)^1\Pi$ level of mixed Rydberg-valence type partially overlap at room temperature). This region necessitates the use of the simulation-fitting technique to determine individual band oscillator strengths. The simulation of these bands is made more difficult by the fact that the corresponding upper states are mixed by relatively strong interactions (Sekine & Hirose 1993). Therefore, they are not pure Σ or Π states, and the degree of mixing has to be determined for each value of the rotational quantum number J in order to determine the intensity of each line. Furthermore, due to isotopic level shifts, the interactions are different in the various isotopomers, leading to different band shapes and intensities. This differs from the case of isolated bands where the band intensity is not expected to vary from one isotopomer to the next. In fact, the concept of band oscillator strength loses its meaning in such cases. Only the line intensities are well defined. Indeed, as shown in Rostas et al. (2000), the band oscillator strengths even become temperature dependent because the mixing coefficients vary with J and the contribution of different J levels to a given band changes with temperature.

The paper is organized in the following way. We describe next the experimental setup for our synchrotron-based measurements. This is followed by the data analysis in Sect. 3 including a brief description of the model describing the mixing of the upper states used to simulate the observed spectra. Section 4 presents our results and a discussion of them and Sect. 5 our conclusions.

2. Experimental setup

The experiments were conducted on the Super-ACO synchrotron ring in Orsay, using the high spectral resolution undulator based SU5 beam line. The VUV spectrometer at this beam line is equipped with a 6.65 m normal incidence concave grating in an off-plane Eagle mounting. Detailed characteristics of the SU5 line and specifications are presented in Nahon et al. (2001a,b). The main features relevant to the wavelength range (900–1080 Å) studied in this work were the use of a SiC grating (2400 lines/mm^{-1}, blazed at 13 eV) in first order, providing a theoretical resolving power of ∼75 000 at 12 eV. Entrance and exit slits of the spectrometer were set either at 35 or 25 μm, giving an instrumental width of 30 or 20 mÅ, respectively. The undulator current was adjusted to optimize the photon flux for each CO band scanned. The undulator was working in the horizontal polarization mode. We verified that the gas filter present on the beam line, used to reject harmonic generation in the undulator, was not necessary in our case. The rotation of the grating was chosen to provide a scanning step of 7 mÅ (about one fourth of the instrumental width). Due to software problems, the automatic translation of the grating was disabled. The grating was positioned in the middle of the range corresponding to each band scanned. Instrumental widths were measured using argon lines at 1048.22 and 894.31 Å as standards. These values were consistent with those deduced from the band-fitting procedure described below.

The VUV light beam emerging from the spectrometer entered a windowless cell system. Several stages of differential pumping were used to maintain the ultra-high vacuum inside the storage ring and the spectrometer. The 30 cm long stage immediately upstream from the gas cell was bounded at each end by a 1.6 mm diameter aperture. The gas cell was adjustable in length (usually 5.4 cm, but 3.5 cm for some bands). High purity $^{12}C^{16}O$ gas (Alphagaz, 99.997%) or $^{13}C^{16}O$ (Eurisotop, 99.1% ^{13}C, 99.95% ^{16}O) or $^{13}C^{18}O$ (Isotech 98.8% ^{13}C, 94.9% ^{18}O) continuously flowed through the cell into the differential pumping section. The pressure in this section, separated from the monochromator chamber by a 1.6 mm aperture, was about 1000 times lower than in the gas cell. The flow was controlled by a needle valve that, once adjusted, maintains a constant pressure in the cell for long periods of time. A 10 Torr full scale capacitor gauge measured the gas pressure in the cell which was generally in the 1–10 mTorr range. Using the 10 mTorr scale, the highest sensitivity for the gauge, leads to measurement uncertainty of ∼0.05 mTorr. Great care was also taken to compensate for zero shifts, through periodic checking of the zero pressure reading. The pressure stability was also monitored by a cold cathode gauge in the differential pumping section where the pressure is in the 10^{-6} Torr range. The flux of synchrotron radiation emerging from the gas cell was measured by a photomultiplier (EMI 9558QB working at −1250 V) by means of fluorescence from a fresh sodium salicylate coating deposited on the glass end-window closing the cell. The PMT anode current was converted to voltage and digitized by a charge amplifier (Keithley type 6485 picoammeter) and then recorded via a GPIB bus on a computer.

To minimize possible errors in the column density arising from weak absorption in the pumping sections and from possible impurities contributing to the total pressure, we used as a standard reference the 3pπ(0) band at 1076 Å, whose oscillator strength is well characterized (Federman et al. 2001). For a given pressure, scans of this band were systematically obtained before and after the scans of the band of interest. The column density derived from these spectra in most cases was in good agreement with that provided by the pressure gauge. Spectral scans of the 967–972 Å region were obtained at 4 different pressures between 2 and 9 mTorr. Several scans were acquired at each pressure as were 2 or 3 scans of the 3pπ(0) reference band. During the course of a set of measurements the pressure was found to vary by 5 to 10%, this leading to corresponding uncertainties in the measurements of the absolute oscillator strength. The scanning step size was usually set at 7 mÅ for the 35 μm slit (or 5 mÅ for the 25 μm slit). The dark current of the PMT was measured before and after each scan by closing a mechanical shutter on the beam line. To take into account the temporal decrease of the beam flux, continuum level (I_0) scans were periodically interspersed within the molecular band records, using the same wavelength range at the same scanning rate as for the adjacent scans but with an empty cell.

3. Data analysis

3.1. The simulation-fitting procedure

After subtraction of the dark current, the recorded intensities are transformed into optical depths using the Beer-Lambert relation, $\tau(\lambda) = \ln (I_0(\lambda)/I(\lambda))$, where $I_0(\lambda)$ and $I(\lambda)$ are the

incident and transmitted intensities respectively. The optical depth $\tau(\lambda)$ is related to the absorption cross section $\sigma(\lambda)$, the column density nl, and the oscillator strength $f(\lambda)$ by the relation $\tau(\lambda) = nl\,\sigma(\lambda) = 8.85 \times 10^{-21}\ \lambda^2\ nlf(\lambda)$, where λ is in Å, n in cm^{-3}, l in cm and σ in cm^2. Changes in the incident intensity I_0, experimentally measured over the course of any one scan, were less than 5%. I_0 was assumed to vary linearly with time (i.e., wavelength) and estimated by a linear interpolation between the intensities recorded at the beginning and the end of the scan.

The corresponding simulated spectrum $\tau(\lambda)$ was calculated, as described below, on the basis of the model established recently by Eidelsberg et al. (2004). For each rotational line, the calculated wavelength and the proper Hönl-London factor (i.e., rotational line strength) were introduced. Each line was convolved with a Voigt profile comprising a Gaussian component corresponding to the room temperature Doppler width and, when appropriate, a Lorentzian component corresponding to the predissociation lifetime of the upper level of the transition.

The optically thin simulated spectrum thus calculated is transformed into an absorption spectrum using the Beer-Lambert law. This spectrum is then convolved with the instrument profile (taken to be Gaussian). As discussed in Eidelsberg et al. (1999) this procedure reproduces the line saturation effects that appear in the experimental spectra when the instrumental width is larger than the spectral line width.

The simulated spectrum is then adjusted to match the experimental spectrum in a non-linear least-squares fitting procedure in which the band oscillator strengths and the instrumental width are free parameters. When predissociation is present, the Lorentzian component can also be left free to adjust in the fit and the resulting value used to determine the predissociation lifetime.

The procedure just described was executed using two independent codes previously applied to derive CO oscillator strengths, one by Federman et al. (1997) for $A-X$ transitions and for the $B-X$, $C-X$, and $E-X$ Rydberg transitions, the other by Eidelsberg et al. (1999) for $A-X$ bands and by Rostas et al. (2000) for intersystem transitions. The agreement in results from the two codes was excellent, typically within 2%.

The procedure was applied first to the 3pπ(0) band used as a standard in order to determine reliable experimental column densities notwithstanding variations in the pressure gradients along the line of sight in the vacuum vessel. The $3p\pi(v' = 0)$ state is far from others and can be considered as practically free of perturbations. Thus, the oscillator strength of the band can be assumed to be the same for CO and its isotopomers $^{13}C^{16}O$ and $^{13}C^{18}O$ (see Stark et al. 1992). The synthetic spectra of this band were calculated using the Hönl-London factors for a $^1\Pi$–$^1\Sigma^+$ transition (Herzberg 1950) and a new set of unpublished line wavelengths extending to $J = 30$ (Eidelsberg et al., unpublished data) obtained through a fit of the available experimental data concerning the $E-X$, $E-A$, $E-B$, and $E-C$ transitions for CO and its isotopomers. The line shape included a Doppler component of 2.5 mÅ and a Lorentzian component of 0.067 mÅ for CO, 0.049 mÅ for $^{13}C^{16}O$, and 0.047 mÅ for $^{13}C^{18}O$ (Cacciani et al. 1998). The Lorentz part of the line width is too small in this case to be determined by the least-squares fit. The rotational temperature was set at 295 K. The column density was obtained by setting the 3pπ(0) band oscillator strength to the value determined by Federman et al. (2001) and by fitting the synthetic 3pπ(0) spectrum to the experimental data. Initially, the instrumental width was allowed to vary. For a given setting of the slits, the inferred width was found to be constant and close to that obtained from the profile of the argon line at 1048 Å. The instrumental width was then kept fixed for a given set of measurements as long as the slits were not changed. Fits were made on the R, P, and Q branches separately and the individual column densities were averaged. A typical fit is shown in Fig. 1 for the 3pπ(0) band in $^{12}C^{16}O$. The absorption cell length was 3.52 cm and the measured pressure 8.4 mTorr. The instrumental width obtained from the fit was 19.6 ± 0.6 mÅ and the column density was (9.75 ± 1.00) × 10^{14} cm^{-2}.

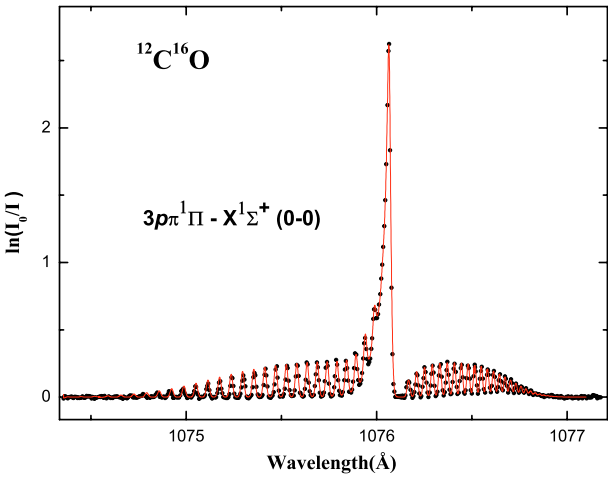

Fig. 1. Fit of the simulated spectrum of the 3p$\pi^1\Pi$(E)–X$^1\Sigma^+$(0–0) to the experimental one for a column density of 9.75 × 10^{14} cm^{-2} and an instrumental width of 19.6 (±0.6) mÅ.

3.2. Calculation of simulated spectra for the perturbed Rydberg transitions

The simulated spectra are calculated taking into account the interactions between the upper states of the four bands. The line positions and the interaction parameters between the states have been determined recently for four isotopomers by Eidelsberg et al. (2004). Proper use of this model allows us to calculate realistic spectra for the bands under study.

The deperturbation analysis by Eidelsberg et al. (2004) shows the upper states of the bands considered here to result from the interaction of the $X^+(0)4p$ complex with the $X^+(1)3d\pi$ component and with the *E(6)* level which is of strongly mixed Rydberg-valence type. The deperturbed molecular parameters and the interaction energies are given in Table 7 of Eidelsberg et al. (2004). These values are introduced in the Hamiltonian energy matrix given in the same reference. Diagonalizing this matrix for each value of J provides the energies of the resulting observed rotational levels $T_i(J)$ and the mixing coefficients $C_{ij}(J)$ that describe the contribution of the deperturbed state j to the mixed wavefunction of state i. As an example the mixing

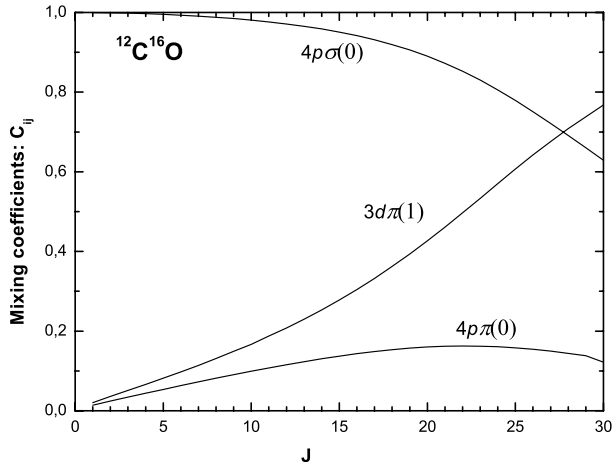

Fig. 2. Mixing coefficient of the 4pσ(0) level in $^{12}C^{16}O$.

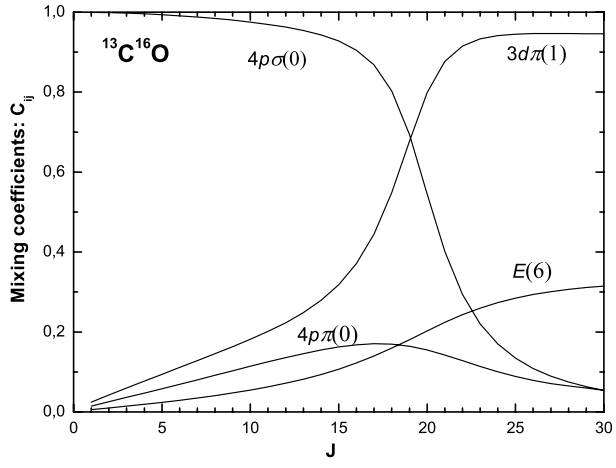

Fig. 3. Mixing coefficient of the 4pσ(0) level in $^{13}C^{16}O$.

coefficients $C_{ij}(J)$ for 4pσ(0) obtained from this procedure are displayed in Figs. 2–4. These figures illustrate the mixing of the 4pσ(0) with the *e* parity levels of the $^1\Pi$ perturbers (l uncoupling). Similar figures for the *e* and *f* parity levels of the $1^1\Pi$, $2^1\Pi$ and $3^1\Pi$ levels which arise from much stronger homogeneous interactions can also be traced.

Following the diagonalization of the energy matrix, the line wavenumbers are calculated as the difference between the energies of the relevant upper and lower levels. The line strengths are obtained as described in Lefebvre-Brion & Field (1986, Eqs. (5.3.29a,b)) which give the perturbed transition amplitudes for transitions between a pair of mutually interacting $^1\Sigma^+$ and $^1\Pi$ upper states and an unperturbed $^1\Sigma^+$ lower state. The expressions for the transition amplitudes include the mixing coefficient, the Hönl-London factor and one perpendicular and one parallel transition moment. Extending these equations to the case of four interacting upper states (three Π and one Σ) leads to the addition of two more transition moments, both of perpendicular type. The Doppler width of CO absorption lines at room temperature, at 970 Å is 2.3 mÅ, which is less than the measured instrumental width of 20 mÅ. For the *L(0)* and *K(0)* bands, the Lorentz part of the line width is even smaller. They were set to the values of Drabbels et al. (1993), i.e.: 1.1 and 0.09 mÅ, respectively, for $^{12}C^{16}O$. For $^{13}C^{16}O$ and $^{13}C^{18}O$, the values given by Cacciani et al. (2002) for *L(0)* were adopted (respectively, 0.7 and 1.7 mÅ); as for the *K(0)* and *E(6)* bands for these isotopomers, 1.7 mÅ was used, corresponding to the lower limit of 3.6×10^{-10} s for the lifetime given by Ubachs et al. (1994). The *L′*(1) band however, is diffuse and the Lorentz component of the width is not negligible. A value of 15 ± 5 mÅ was found through our fits and was used for all three isopotomers.

The calculated spectra are fitted to the experimental ones using a nonlinear least-squares method. This procedure yields integrated cross sections for each of the bands involved, independently of their overlap. A test of the quality of the process is provided by the fact that the sum of the integrated cross sections of the three bands should be the same for the three isotopomers.

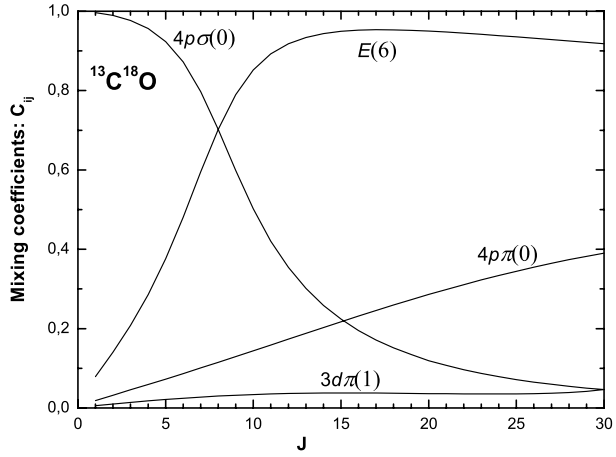

Fig. 4. Mixing coefficient of the 4pσ(0) level in $^{13}C^{18}O$.

4. Results and discussion

The band system in the 967–972 Å range was scanned for the three isotopomers, $^{12}C^{16}O$, $^{13}C^{16}O$ and $^{13}C^{18}O$, at several pressures in the 1 to 10 mTorr range. Figures 5–7 illustrate typical results for each of the three isotopomers. In these figures and from now on the observed mixed levels of $^1\Pi$ symetry are referred following the notation of Eidelsberg et al. (2004), as $1^1\Pi$, $2^1\Pi$ and $3^1\Pi$, in order of increasing energy. In each figure, trace (a) represents the calculated spectra of the individual bands, (b) the sum of these spectra, c) the experimental spectrum and (d) the residuals obs-calc. The model reproduces the evolution of the spectrum when going from one isotopomer to the next very well.

The fitting procedure provides, for a given spectrum, the oscillator strengths of each component band. The results of the present study are given in Tables 1–3 with a comparison to others that are available. The oscillator strength for a given band varies from one isotopomer to the next because the amount of mixing between bands differs. However, the total oscillator strength of the band system should not be isotope sensitive as it is the sum of those of the deperturbed bands which themselves are not sensitive to isotope effects. This expectation is verified within about 10% and provides a good test of the overall

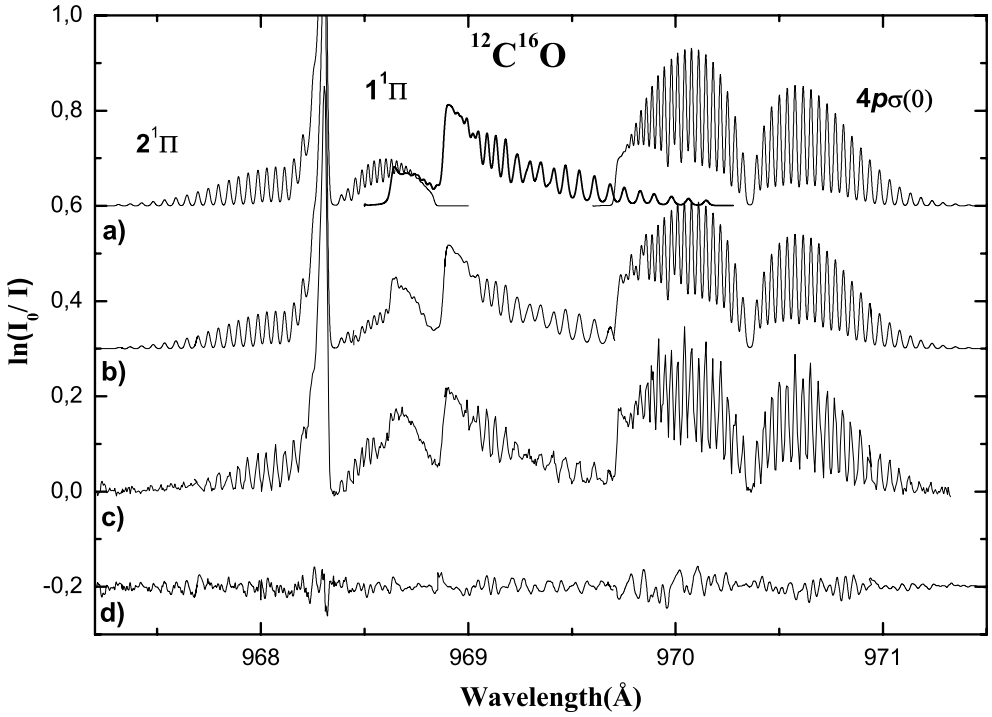

Fig. 5. a) Simulated spectra of the 3 bands $1^1\Pi$–X, $2^1\Pi$–X and 4pσ(0)–X in $^{12}C^{16}O$ taking into account the l uncoupling interaction between the two $1^1\Pi$ levels with the $X^+(0)4p\sigma$ level. **b)** Fit of the 3 bands together. **c)** Experimental spectra for a column density of 9.75×10^{14} cm^{-2} and an experimental width of 20 mÅ. **d)** Quality of the fit.

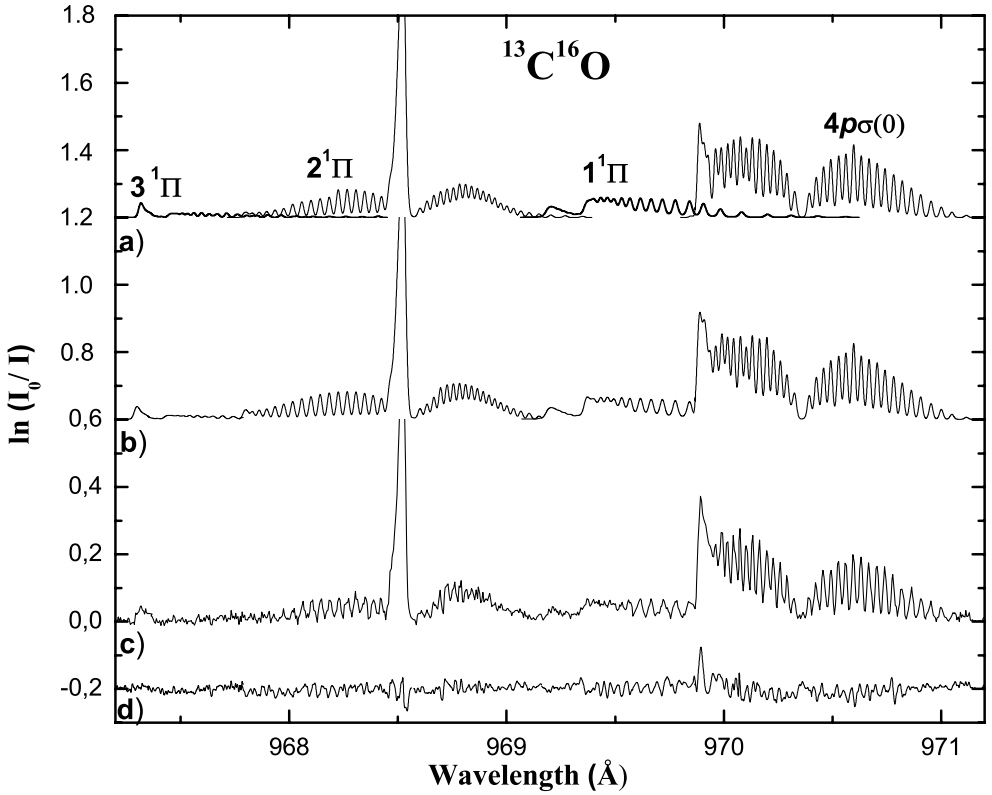

Fig. 6. a) Simulated spectra of the 4 bands $3^1\Pi$–X, $2^1\Pi$–X, $1^1\Pi$–X, and 4pσ(0)–X in $^{13}C^{16}O$ taking into account the l uncoupling interaction between the 4pσ(0) level with the 4pπ(0) level, and the homogeneous interactions of the 4pπ(0) and 3dπ(1) levels with the *E(6)* perturber. **b)** Fit of the 4 bands together. **c)** Experimental spectra for a column density of 7.8×10^{14} cm^{-2} and an experimental width of 20 mÅ. **d)** Quality of the fit.

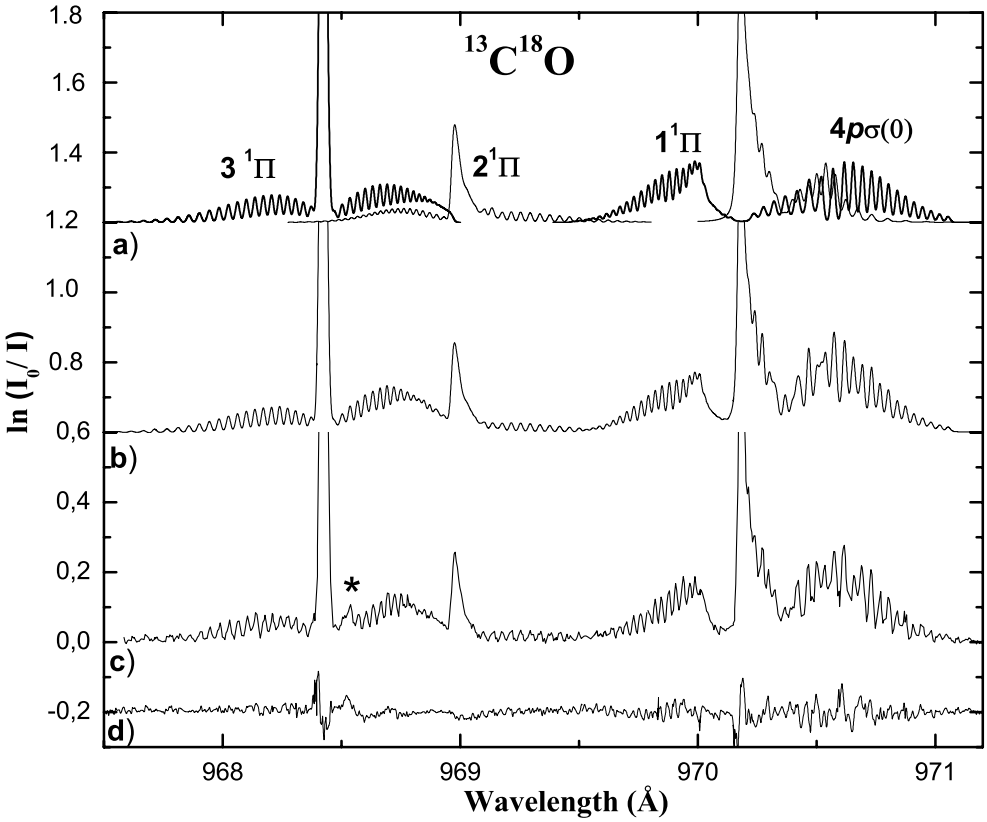

Fig. 7. a) Simulated spectra of the 4 bands $3^1\Pi$–X, $2^1\Pi$–X, $1^1\Pi$–X, and 4pσ(0)–X in in $^{13}C^{18}O$ taking into account the l uncoupling interaction between the 4pσ(0) level with the 4pπ(0) level, and the homogeneous interactions of the 4pπ(0) and 3dπ(1) levels with the *E(6)* perturber. **b)** Fit of the 4 bands together. **c)** Experimental spectra for a column density of 9.75×10^{14} cm^{-2} and an experimental width of 20 mÅ. **d)** Quality of the fit. The asterisk $*$ indicates a contamination of the P branch by the Q branch of the same transition in $^{13}C^{16}O$.

Table 1. Oscillator strengths for $^{12}C^{16}O$ bands between 967 and 972 Å (f-values $\times 10^{-3}$).

Band	Band Origin	This work	Letzelter et al. (1987)*	Stark et al. (1991)*	Stark et al. (1993)*	Stark et al. (1993)*	Yoshino et al. (1995)*	Sheffer et al. (2003)
(upper level)	λ_0 (Å)	**295 K**	**295 K**	**295 K**	**295 K**	**20 K**	**20 K**	**ISM**
4pσ(0)[a]	970.357	34.1 ± 3.4	21.0 ± 2.1	13.4 ± 1.3	26.0 ± 2.6	26.8 ± 5.3	33.5 ± 5.0 34.8[b]	31 ± 4 35.0[c]
$1^1\Pi$[a]	968.889	12.0 ± 1.2	12.4 ± 1.2	8.5 ± 0.8	⎤ 22.4 ± 2.4	11.4 ± 2.3	...	10.1 ± 1.1 11.19[c]
$2^1\Pi$[a]	968.300	14.5 ± 1.5	7.7 ± 0.8	>8.9	⎦	7.5 ± 0.8	11.9 ± 1.8 13.85[b]	...
4pσ(0) + $1^1\Pi$ + $2^1\Pi$	...	60.6 ± 6.1	41.1	>30.8	48.4	45.7	...	...

* For comparison, the integrated absorption cross sections given in these references have been transformed into oscillator strengths through the relation $f = (113 \times \int \sigma(\lambda)\, \mathrm{d}\lambda)/\lambda^2$, where the cross section $\sigma(\lambda)$ is in 10^{-18} cm^2 and λ is in Å.
[a] 4pσ(0), $1^1\Pi$ and $2^1\Pi$ refer to K, L and L', respectively, in the old notation.
[b] Our calculated value at 20 K.
[c] Our calculated value at 4 K.

quality of our results which depends both on the model used and on the experimental procedure.

The present results are also compared to previous ones in Tables 1–3. The comparison is straightforward for other data recorded at room temperature. However, the data of Stark et al. (1993) and Yoshino et al. (1995) obtained at 20 K and the 4 K interstellar (ISM) data of Sheffer et al. (2003) cannot, in principle, be compared directly. Instead, we recalculated synthetic spectra for 20 and 4 K and obtained band oscillator strengths for comparison with the values shown in Table 1. The agreement between our inferred oscillator strengths and the recent determinations (Yoshino et al. 1995; Sheffer et al. 2003) is excellent, being within the quoted 1-σ empirical uncertainties. The band values previously obtained experimentally at room temperature without the help of the fitting technique are somewhat arbitrary due to the overlaps. Therefore, only the oscillator strengths for the total band system are comparable. Our room temperature results tend to be about 50% larger than the

Table 2. Oscillator strengths for $^{13}C^{16}O$ bands between 967 and 972 Å (f-values $\times 10^{-3}$).

Band (upper level)	Band origin λ_0 (Å)	This work	Eidelsberg & Rostas (1990)
$4p\sigma(0)^a$	970.356	32.64 ± 3.26	18.30 ± 1.83
$1^1\Pi^a$	969.359	6.99 ± 0.70	11.42 ± 1.14
$2^1\Pi^a$	968.532	20.72 ± 2.07	12.77 ± 1.28
$3^1\Pi^a$	967.426	1.20 ± 0.12	
$4p\sigma(0) + 1^1\Pi + 2^1\Pi + 3^1\Pi$	...	61.55 ± 6.16	42.49 ± 4.25

[a] $4p\sigma(0)$, $1^1\Pi$ and $2^1\Pi$ refer to K, L' and L, respectively, in the old notation, while $3^1\Pi$ corresponds to the newly characterized *E(6)*.

Table 3. Oscillator strengths for $^{13}C^{18}O$ bands between 967 and 972 Å (f-values $\times 10^{-3}$).

Band (upper level)	Band origin λ_0 (Å)	This work
$4p\sigma(0)^a$	970.365	22.32 ± 2.23
$1^1\Pi^a$	970.139	20.90 ± 2.09
$2^1\Pi^a$	968.964	5.57 ± 0.56
$3^1\Pi^a$	967.529	18.06 ± 1.80
$4p\sigma(0) + 1^1\Pi + 2^1\Pi + 3^1\Pi$	...	66.85 ± 6.69

[a] $4p\sigma(0)$, $2^1\Pi$ and $3^1\Pi$ refer to K, L' and L, respectively, in the old notation, while $1^1\Pi$ corresponds to the newly characterized *E(6)*.

previous ones, for both $^{12}C^{16}O$ and $^{13}C^{16}O$. This could be attributed to possible optical depth effects which might have affected earlier results (see also Federman et al. 2001).

5. Conclusions

We carried out absorption experiments using synchrotron radiation to measure oscillator strengths for several overlapping Rydberg transitions in $^{12}C^{16}O$, $^{13}C^{16}O$ and $^{13}C^{18}O$. In this paper particular attention was devoted to the *L(0)*, $L'(1)$, and *K(0)* bands of all three isotopomers as well as the *E(6)* band in the two rarer forms of CO. The necessary line strengths and mixing coefficients were obtained from the deperturbed molecular parameters given in Eidelsberg et al. (2004).

As for the bands at wavelengths greater than 1075 Å, consensus is emerging regarding oscillator strengths for the *L(0)*, $L'(1)$, and *K(0)* bands of $^{12}C^{16}O$; our results are consistent with other recent determinations. This consistency among results for $^{12}C^{16}O$ and the fact that the sum of oscillator strengths for the set of overlapping bands is independent of isotopomer give us confidence in our results on $^{13}C^{16}O$ and $^{13}C^{18}O$. Since absorption involving these bands plays an important role in CO photodissociation in astronomical environments (e.g., van Dishoeck & Black 1988), use of our larger oscillator strengths for $^{12}C^{16}O$ and $^{13}C^{16}O$ and our new ones for $^{13}C^{18}O$ may help resolve the differences now found between model predictions and observations (e.g., see Sheffer et al. 2003; Federman et al. 2003).

Acknowledgements. The authors are obliged to Joelle Rostas for useful discussions and to K. P. Huber for critically reading the manuscript and for his suggestions. They also acknowledge the support of the LURE-Super ACO facility and the SU5 beam line team. This research was funded in part by the CNRS-PCMI program and NASA grant NAG5-11440.

References

Cacciani, P., Ubachs, W., Hinnen, P. C., et al. 1998, ApJ, 499, L223
Cacciani, P., Brandi, F., Sprengers, J. P., et al. 2002, Chem. Phys., 282, 63
Drabbels, M., Heinze, J., ter Meulen, J. J., & Meerts, W. 1993, J. Chem. Phys., 99, 5701
Eidelsberg, M., Launay, Le Floch, A., & Rostas, J., unpublished
Eidelsberg, M., & Rostas, F. 1990, A&A, 235, 472
Eidelsberg, M., Jolly, A., Lemaire, J. L., et al. 1999, A&A, 346, 705
Eidelsberg, M., & Rostas, F. 2003, ApJS, 145, 89
Eidelsberg, M., Launay, F., Ito, K., et al. 2004, J. Chem. Phys., 121, 292
Federman, S. R., Menningen, K. L., Lee, W., & Stoll, J. B. 1997, ApJ, 477, L61
Federman, S. R., Fritts, M., Cheng, S., et al. 2001, ApJS, 134, 133
Federman, S. R., Lambert, D. L., Sheffer, Y., et al. 2003, ApJ, 591, 986
Herzberg, G. 1950, Molecular spectra and molecular structure (D. van Nostrand Company, Inc. Princeton), 208
Lefebvre-Brion, H., & Field, R. 1986, Perturbations in the spectra of diatomic molecules (Academic Press Inc.), 273
Letzelter, C., Eidelsberg, M., Rostas, F., Breton, J., & Thieblemont, B. 1987, Chem. Phys., 14, 273
Nahon, L., Polack, F., Lagarde, B., et al. 2001, NIMPA, 467, 463
Nahon, L., Alcaraz, C., Marlats, J. L., et al. 2001, Rev. Sci. Instr., 72, 1320
Rostas, F., Eidelsberg, M., Jolly, A., et al. 2000, J. Chem. Phys, 112, 4591
Sekine, S., & Hirose, C. 1993, Chem. Phys. Lett., 212, 129
Sheffer, Y., Lambert, D. L., & Federman, S. R. 2002, ApJ, 574, L171
Sheffer, Y., Federman, S. R., & Andersson, B.-G. 2003, ApJ, 597, L29
Stark, G., Yoshino, K., Smith, P. L., Ito, K., & Parkinson, W. H. 1991, ApJ, 369, 574
Stark, G., Smith, P. L., Ito, K., & Yoshino, K. 1992, ApJ, 395, 705
Stark, G., Yoshino, K., Smith, P. L., et al. 1993, ApJ, 410, 837
Ubachs, W., Eikema, K. S. E., Levelt, P. F., et al. 1994, ApJ, 427, L55
van Dishoeck, E. F., & Black, J. H. 1988, ApJ, 334, 771
Yoshino, K., Stark, G., Esmond, J. R., et al. 1995, ApJ, 438, 1013